ELSEVIER

Earth and Planetary Science Letters 204 (2002) 47–60

EPSL

www.elsevier.com/locate/epsl

Suppression of large-scale magma mixing by melt–volatile separation

Jeremy C. Phillips [a,*], Andrew W. Woods [b]

[a] *Centre for Environmental and Geophysical Flows, Department of Earth Sciences, University of Bristol, Bristol BS8 1RJ, UK*
[b] *BP Institute for Multiphase Flow, University of Cambridge, Cambridge CB3 0EZ, UK*

Received 16 April 2002; received in revised form 6 September 2002; accepted 19 September 2002

Abstract

Many volcanic eruptions are triggered by the injection of hot basic magma into a subsurface reservoir containing cooler and less dense silicic magma. As the basaltic magma cools and crystallises, it may become volatile saturated and exsolve bubbles. Here we present a new quantitative model and supporting laboratory experiments which identify that if a sufficient number of bubbles remain in suspension, then the bulk density of the basalt may fall below that of the silicic magma. However, if the basalt has sufficiently low viscosity, or the cooling rate is sufficiently small, then the bubbles can rise through the basalt, suppressing the large-scale overturn, and forming an intermediate bubbly layer at the interface with the more viscous silicic magma. As the small bubble plumes then rise from this foam and transport vesicular basalt into the upper layer, the chamber now remains density stratified.

Keywords: magma mixing; volatiles; bubbles; convection; overturn

1. Introduction

When juvenile magma is intruded into the base of an existing magma chamber in the crust, it begins to cool, crystallise and convect. Typically the intruded magma is dense and ponds below the evolved, viscous magma already in the chamber [1–3]. As the lower layer crystallises, the magma becomes saturated and volatile bubbles are exsolved. If all the bubbles remain in the lower convecting layer, then the density of this layer may fall below that of the overlying magma and large-scale overturn of the two magma bodies may ensue [3–7]. However, if the bubbles rise out of the basalt, they can form a foam at the interface [8,4]. Since the foam is bubble-rich, it will be less dense than the overlying liquid and a series of plumes will rise from the foam into the upper layer, mixing small inclusions of the juvenile magma into the more evolved, overlying magma [1,4,8–10] although there is no large-scale overturn of the system. This mechanism enables exsolved volatiles resulting from recent recharge to accumulate at higher levels in the magma cham-

* Corresponding author. Tel.: +44-117-954-5241; Fax: +44-117-925-3385.
E-mail addresses: j.c.phillips@bristol.ac.uk (J.C. Phillips), andy@bpi.cam.ac.uk (A.W. Woods).

0012-821X/02/$ – see front matter
PII: S0012-821X(02)00978-0

ber, possibly leading to elevated volcanic gas emissions [10,11].

Geological evidence [1,5–7,9] suggests that each of these mixing processes can occur in magma reservoirs. The former may be manifest in the eruption of mixed and co-mingled magmas [5,7], while the latter is manifest in the eruption of evolved magma containing inclusions of the newly intruded magma [1,6]. Here we develop a new theoretical model with supporting laboratory experiments in order to establish some of the principles that control which of these two regimes may arise. We first develop a model of the density evolution of the basalt as it cools and crystallises beneath a layer of silicic magma, which is heated by the basalt. We account for the change in pressure of the chamber as the density of each layer evolves [12]. Initially, we neglect the effects of bubble separation from the convecting magma to establish conditions under which overturn could occur. Our calculations suggest that a reversal in bulk density of the two layers prior to eruption is most likely in relatively shallow chambers in which both the silicic and basaltic layers are saturated in volatiles. We then extend the model to examine the potential role of bubble–magma separation in suppressing such an overturn. We establish that if the rate of bubble separation from the lower basaltic layer exceeds the rate of bubble production through cooling and crystallisation, then the large-scale overturn of the two magmas may be suppressed. We then present a series of new analogue laboratory experiments, in which we verify that bubble–magma separation from the lower layer may suppress the large-scale overturn of the layers, in accord with our model predictions. Our experiments also indicate that if large-scale overturn is suppressed, then plume-driven mixing from the interfacial foam is still able to generate some mixing of the layers [4]. We then briefly discuss the application of our results to specific historical eruptions.

It is worth stating at the outset that the main focus of our work is to identify some of the physical balances which arise during the evolution of two cooling and crystallising magmas in which there are also exsolved volatiles. Our approach is to take typical values, derived from the literature, for various properties and processes, which illustrate the magnitude and typical evolution of the magma as it cools and crystallises. We then use these in the model to explore conditions under which different general styles of behaviour may arise. In our calculations, we have used simplified parameterisations for the volatile exsolution and the crystal production on cooling, which are consistent with the general form of previously published laboratory experiments and theoretical studies on magmas [4,8,13–15]. We comment on the limitations of this approach and the detailed parameterisations required to simulate specific volcanic eruptions in the discussion.

2. Density evolution in absence of bubble separation

We now explore the density evolution of a chamber in which the lower layer cools, crystallises and becomes volatile saturated, assuming that the layer is well-mixed by bubble convection ([8]; Appendix A). We first examine the evolution of the densities of each layer as heat is transferred from the basaltic to the silicic magma, assuming that there is no separation of bubbles from the melt. We illustrate conditions under which the density of the basalt may decrease to that of the silicic magma and trigger large-scale overturn and mixing. We then examine the role of bubble separation from the magma, to explore how this reduces the density decrease of the basalt and may thereby suppress overturn.

We examine the density evolution of a magma chamber in which a basaltic layer of mass M_b, temperature T_b, crystal content x_b, and total gas content N_b underlies a silicic layer of mass M_s, temperature T_s, crystal content x_s and total gas content N_s (Fig. 1). We assume that the two bodies of magma lie in a chamber of volume V, and that the bulk modulus of the wall-rock and melt β_w and β_m, taken to have values 10^{11} and 10^{10} Pa, respectively [16]. We take the initial pressure of the chamber to be p.

In order to develop some quantitative understanding of the evolution of the system, we re-

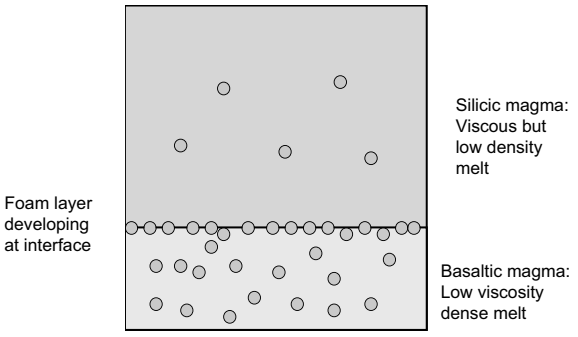

Fig. 1. Schematic of the two-layer magma reservoir, with dense basaltic magma underlying an evolved layer of silicic magma.

quire some parameterisations of the different physical properties of the magma [2,12]. The mass of gas dissolved in the melt depends on the pressure and the melt fraction according to Henry's law, which may be represented by the approximate form:

$$n_i = s_i p^{1/2}\,(1-x_i) \tag{1}$$

where $i = s$ or b, denoting silicic or basaltic magma. Representative values for the solubility constants for the silicic and basaltic magmas are $s_s = 4\times10^{-6}$ and $s_b = 3\times10^{-6}$ $\mathrm{Pa}^{1/2}$, respectively [17]. The crystal content of the basaltic and silicic magmas may be approximated by the simple relations [18]:

$$x_s = (T_s - 800)/150 \text{ and } x_b = (1200 - T_b)/200 \tag{2}$$

The change in pressure of the system results from the change in temperature of the two bodies of magma and the associated change in the mass of exsolved volatiles. This changes the bulk density of both the basaltic and silicic magmas and hence the pressure in the chamber. The bulk density of each layer of magma is given by the relation:

$$\rho_i = \left(\frac{(N_i - n_i)RT_i}{p} + \frac{1-(N_i-n_i)}{\sigma_i}\right)^{-1} \tag{3}$$

where σ_i is the bulk density of the melt and crystal mixture, given by:

$$\sigma_i = \left(\frac{1-x_i}{\rho_{mi}} + \frac{x_i}{\rho_{ci}}\right)^{-1} \tag{4}$$

Here ρ_{ci} is the density of the crystals produced from layer i, taken to have a typical value 2800 $\mathrm{kg/m^3}$ in basalt and 2600 $\mathrm{kg/m^3}$ in silicic magma at a pressure of 150 MPa. ρ_{mi} is the density of the melt phase i, taken to have the representative value $\rho_{ms} = 2300$ $\mathrm{kg/m^3}$ for the silicic magma and $\rho_{mb} = 2600$ $\mathrm{kg/m^3}$ for the basaltic magma.

Owing to the convection in both layers ([2]; Appendix A), we assume the main heat transfer occurs between the basaltic and silicic magmas, leading to cooling and crystallisation of the basalt and heating and resorption of crystals in the silicic magma. In the absence of significant heat losses to the walls of the chamber, the conservation of heat requires that the decrease in thermal energy of the basalt matches the increase of thermal energy in the silicic magma:

$$M_b\left(C_p + L_b\frac{dx_b}{dT}\right)\frac{dT_b}{dt} = -M_s\left(C_p + L_s\frac{dx_s}{dT}\right)\frac{dT_s}{dt} \tag{5}$$

where dT_i/dt is the rate of change of temperature of the magma i, with $i = s$ or b, and where L_i denotes the latent heat of crystallisation [12]. As the magma cools and crystallises, the overall density and hence volume of magma in the chamber, V, evolves. This leads to a change in pressure p, owing to the deformation of the country rock [19]:

$$\beta_w dV/dt = V\,dp/dt \tag{6}$$

The change in volume may also be related to the change in density of the upper and lower layers, since the total volume of the chamber may be written in the form:

$$V = \left(\frac{M_b}{\rho_b} + \frac{M_s}{\rho_s}\right) \tag{7}$$

Combining Eqs. 5–7, it follows that the rate of change of pressure, dp/dt, may be related to the

rate of cooling of the basaltic magma, dT_b/dt, according to the relation:

$$\left(\frac{V}{\beta_w}+\frac{M_b}{\rho_b^2}\frac{\partial\rho_b}{\partial p}+\frac{M_s}{\rho_s^2}\frac{\partial\rho_s}{\partial p}\right)\frac{dp}{dt}=$$

$$-\left(\frac{M_b}{\rho_b^2}\frac{\partial\rho_b}{\partial T}+\frac{M_s}{\rho_s^2}\frac{dT_s}{dT_b}\frac{\partial\rho_s}{\partial T}\right)\frac{dT_b}{dt} \quad (8)$$

We can thereby predict the evolution of the density of both the silicic and basaltic magmas as a function of the temperature or crystal content (Eq. 2) of the basaltic magma. Snyder [15] showed that the pressurisation generated by exsolution of water from a silicic melt due to heating is suppressed above a few hundred MPa. The applicability of this model is thus limited to magma chamber pressures less than about 300 MPa, although we note this includes recent volcanic eruptions such as Mount St. Helens, Pinatubo, Soufriere Hills Montserrat and Unzen [15].

Our model is analogous to that presented by Folch and Marti [12], but here we focus on the density evolution of each of the layers of magma and the ability of the magmas to overturn. There are a number of parameters which influence the density evolution of each layer. One important control is the compressibility of the upper silicic layer which occupies the major part of the chamber. If the upper layer is volatile saturated, then it will be relatively compressible and a decrease in the density of the basalt may be accommodated with relatively little change in chamber pressure (cf. [20]). Hence, the chamber may evolve towards conditions in which overturn is possible before the chamber pressure has become so elevated that it triggers an eruption. Conversely, if the silicic layer remains volatile unsaturated, then it is relatively incompressible and the chamber pressure increases much more rapidly owing to expansion of the basalt as it cools, crystallises and exsolves volatiles. In this case, the chamber pressure may increase sufficiently to trigger eruption prior to any density reversal. To illustrate these effects we present two sets of calculations in Figs. 2 and 3.

Fig. 2 illustrates how the density and pressure of the basaltic and silicic magmas evolve, assuming that the bubbles and crystals remain in suspension and well-mixed in the layer of magma in which they form. Fig. 2 corresponds to a basaltic layer containing 3 wt% volatiles and with no initial crystals, and a silicic layer which is 40% crystalline, containing (a) 4 wt%, (b) 3 wt% and (c) 2 wt% volatiles. The more volatile rich silicic magma (case a) is volatile saturated, and therefore quite compressible. Initially, as the basalt cools

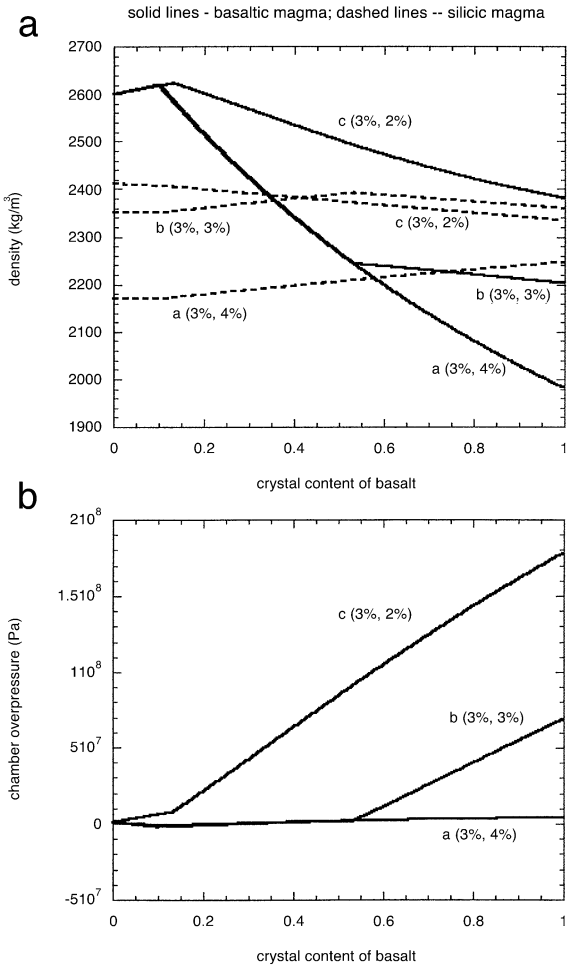

Fig. 2. Model calculations of (a) the density of the basaltic (solid) and silicic (dashed) layers of magma, and (b) the chamber pressure, in a 5-km-deep chamber, as a function of the crystal content of the basalt. In the calculations, the chamber volume is 10 km^3, the basaltic magma occupies 10% of the chamber volume, and the initial temperatures of the basalt and silicic magmas are 1300 and 800°C. As indicated in the different lines, the basalt is assumed to have 3 wt% volatiles, while the silicic magma has (a) 4 wt%; (b) 3 wt% and (c) 2 wt%.

and crystallises, it is volatile undersaturated, and the formation of dense crystals increases the bulk density of the basalt (Fig. 2a). However, it becomes volatile saturated when it has a crystal mass fraction of about 0.1, and subsequently its density falls, until dropping below that of the silicic magma, when it has a crystal content of about 0.6. At this stage, the simple model would suggest overturn of the two layers of magma. As the basalt cools, the silicic magma heats up and resorbs some crystals and volatiles. As a result, the density of the silicic magma increases gradually. There is relatively little change in the chamber pressure since it is highly compressible owing to the presence of bubbles in the silicic magma (Fig. 2b). In case b, the silicic magma is assumed to have only 3 wt% volatiles, and so in this case, the silicic magma is initially denser owing to the smaller mass of exsolved gas, and overturn is predicted at a crystal content in the basalt of about 0.35. We have in fact continued our calculations beyond this point, neglecting any effects of the overturn; our calculations show that when the basalt reaches a crystal content of about 0.55, the silicic magma has resorbed all the exsolved gas initially in the silicic layer. The silicic layer then becomes much less compressible, and any subsequent heating of the silicic magma leads to expansion of the silicic magma through resorption of the dense crystals. As a result, the chamber pressure begins to increase rapidly, and the density of the basaltic layer falls more gradually because of the increase in solubility of the gas and in the density of the bubbles. In case c, the silicic magma has only 2 wt% volatiles, and remains unsaturated in volatiles. As a result, the chamber is highly incompressible. Once the basalt becomes volatile saturated, at a crystal content of about 0.1, the density of the basalt falls off much more slowly owing to the rapidly increasing chamber pressure, as in case b. In case c, overturn does not occur because the density of the basalt in fact remains greater than that of the silicic magma; by comparison with cases a and b, we deduce that this is largely a consequence of the fact that the silicic magma is unsaturated and hence relatively incompressible, so that the chamber pressure increases rapidly as the basalt starts to exsolve volatiles. Indeed, the level of overpressure calculated in Fig. 2b are unrealistically high, and we expect eruption to occur soon after the basalt begins to exsolve volatiles. In contrast, for the volatile saturated case a, there is relatively little change in the chamber pressure, and overturn may occur.

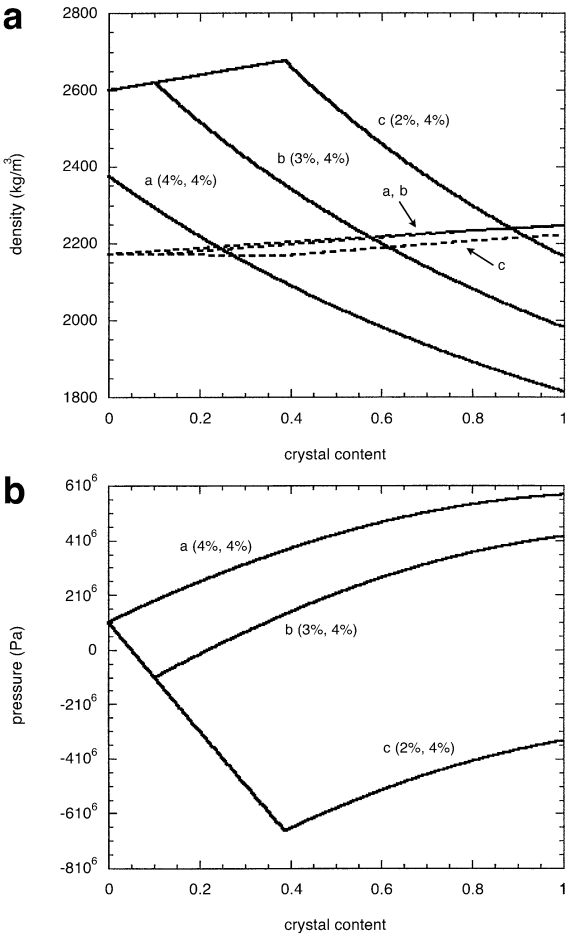

Fig. 3. Model calculations of (a) the density of the basaltic (solid) and silicic (dashed) layers of magma, and (b) the chamber pressure, in a 5-km-deep chamber, as a function of the crystal content of the basalt. In the calculations, the chamber volume is 10 km^3, the basaltic magma occupies 10% of the chamber volume, and the initial temperatures of the basalt and silicic magmas are 1300 and 800°C. As indicated in the different lines, the silicic magma is assumed to have 4 wt% volatiles, while the basaltic magma has (a) 4 wt%; (b) 3 wt% and (c) 2 wt%.

Fig. 3 illustrates the influence of the volatile content of the basaltic magma on the develop-

ment of overturn. We present the evolution of the density and the chamber pressure as a function of the crystal content of the basalt for basaltic magma with (a) 4 wt%, (b) 3 wt% and (c) 2 wt% volatiles, underlying a layer of silicic magma with 4 wt% volatiles and an initial crystal content of 0.4. Note that these volatile contents are the *total* volatile content (not the dissolved volatile content) and the values we have used are representative of the range observed in natural samples [21,22]. In case (a), the basalt is volatile saturated before it begins to cool and crystallise, and so once crystallisation begins, the density of the basalt decreases through further bubble production. Overturn with the silicic magma is then predicted once the crystal content exceeds a mass fraction of about 0.25. For cases (b) and (c), the basalt remains unsaturated in volatiles until a finite mass of the magma has crystallised. Therefore, initially the density of the basalt increases, but once the basalt becomes volatile saturated, the density begins to decrease, and we predict overturn at somewhat larger crystal fractions. Although we present graphs for crystal content increasing to values of order 1.0, the model will cease to hold for crystal content in excess of about 0.6, when the basalt ceases to behave as a fluid. In case (a), the chamber pressure gradually increases owing to the bubble formation in the basalt, even though the density of the silicic magma gradually increases through resorption of exsolved volatiles as it is heated. In cases (b) and (c), the pressure actually falls during the early phase of crystallisation of the basalt, while it is volatile unsaturated. However, the system is repressurised once volatiles begin to be exsolved in the basalt.

3. Effect of bubble–magma separation

The above predictions of some of the controls on overturn represent an extension of the work of Huppert et al. [2], in which the chamber pressure was assumed to remain constant during the crystallisation. The main advance is the recognition that if the silicic layer is volatile unsaturated, then it is highly incompressible. As a result, we find that as the basalt expands through exsolution of volatiles, the chamber pressure builds up very rapidly and an eruption may be triggered before magma overturn occurs (Fig. 2).

However, since the basalt is of relatively low viscosity it is possible that some of the bubbles rise out of the basalt [23], and some of the crystals settle from the basalt [24], thereby changing the bulk density of the lower layer. Both of these processes may also have an important impact on the ability of the system to overturn, and we now explore this in more detail.

Cardoso and Woods [23] established experimentally that in a turbulently convecting liquid, bubble loss (volume flux) occurs at a rate $-v_b\, A\phi$ where A is the chamber cross-section, v_b the bubble rise speed, and ϕ is the volume fraction of the magma occupied by bubbles. We may include this loss of bubbles and crystals from the layer of basalt in the above model, through an equation of the form:

$$d\phi_b/dt = \Phi - v_s\phi_b/h_b \tag{9}$$

where:

$$\Phi = \frac{d}{dt}\left(\frac{\rho_b RT}{p}\,(N_b - n_b)\right) \tag{10}$$

is the production rate of bubbles per unit volume associated with the cooling and crystallisation, ϕ_b denotes the bubble volume fraction of the lower layer, and h_b is the depth of the lower layer. By combining Eq. 10 with the model for the cooling and crystallisation presented in the previous section, we have made some revised predictions of the density evolution of the basalt. For simplicity, in the present work we assume that the bubbles in the silicic layer remain in suspension, as that layer is typically much more viscous; however, in the later section concerning our laboratory experiments, we show that this simplification does not affect our main conclusions.

Before presenting the results of our calculations, we first examine the time-scale for bubble separation relative to that of cooling. If the time-scale for bubbles to separate from the melt, h/v_s, is shorter than the cooling time over which bubbles are produced, then the bubbles will not be effec-

tive in reducing the bulk density of the basalt. For bubbles of size 10–50 μm, the rise speeds in basalt, of viscosity 10–100 Pa, will lie in the range 10^{-8}–10^{-6} m/s [13]. The time-scale for bubble loss, h/v_s, in a layer of depth $h \sim 10$–100 m, will therefore lie in the range 10^{7}–10^{10} s. This may be comparable to the typical cooling time of the basalt, which lies in the range 10^{7}–10^{11} s for a 10–100-m-deep layer, depending on the efficiency of convective cooling. Therefore, we anticipate that, in some cases, bubble separation might be important in suppressing overturn of the two layers of magma.

To illustrate the effect of bubble separation, in Fig. 4 we present two different calculations which indicate how the density of the basaltic layer evolves if bubbles are able to separate from this layer according to Eq. 9. In Fig. 4a, we present a calculation corresponding to case b of Fig. 2, in which both layers have 3 wt% volatiles, and a cooling rate of 10^{-6} K/s of the basalt is used. Dashed curves show the bulk density of the basalt for bubble rise speeds of 10^{-7} m/s and 5×10^{-7} m/s, in comparison to the case of no bubble separation. It is seen that with the higher bubble rise speed, the density of the basalt actually remains greater than that of the silicic magma, and so in this case bubble separation is able to suppress overturn. However, for the smaller rise speed, there is insufficient bubble separation to suppress the overturn. Similarly, in Fig. 4b we illustrate how the density of the basalt is affected by bubble separation for case a of Fig. 3, in which both layers of magma have 4 wt% volatiles. In this case, we assume a cooling rate of the basalt of 10^{-7} K/s, and the figure illustrates that overturn may be suppressed if the bubble rise speed is of order 3×10^{-8} m/s. These two figures illustrate that bubble separation can suppress overturn if the bubble rise time is sufficiently short compared to the cooling time.

In making these calculations, we have assumed that the crystals remain in suspension in the basalt. Although the density difference between the crystals and magma is likely to be smaller than that between the bubbles and the magma, crystals may settle from the basalt [24,25]. Crystal settling can lead to a decrease in the density of the resid-

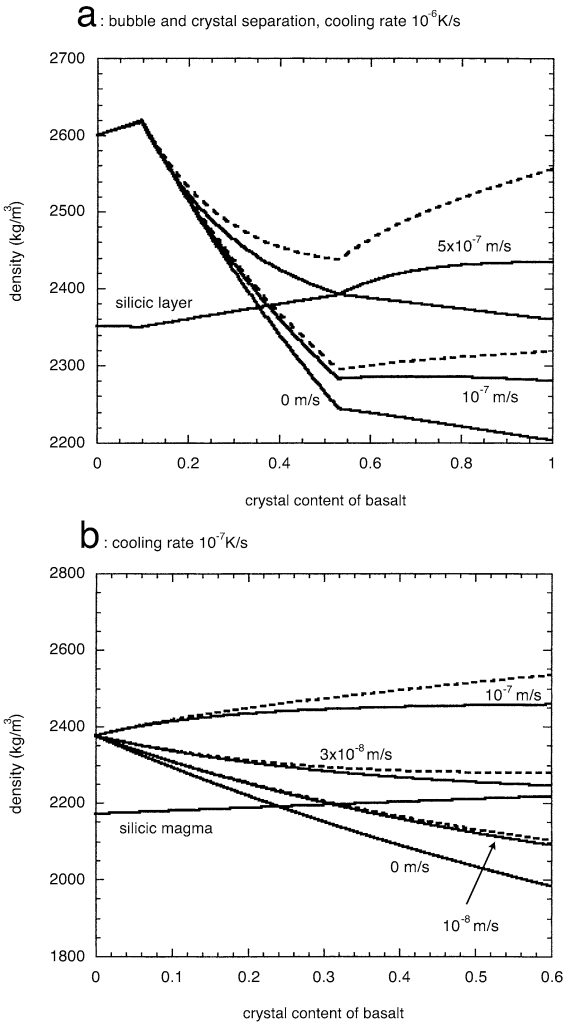

Fig. 4. Model calculations showing the effect of bubble and crystal separation in the basalt on the density evolution of the magma as a function of the mass fraction of crystals formed from the basalt. The solid curves correspond to the density of the basalt, assuming that bubble rise speed equals the crystal fall speed; the dashed curves correspond to the density of the basalt assuming that the crystals all remain suspended in the melt, and the dotted curve corresponds to the density of the silicic magma. In a, the simulation corresponds to the case b of Fig. 2, with 3 wt% volatiles in both the silicic magma and the basaltic magmas, and we now assume a cooling rate of 10^{-6} K/s. Curves are given for bubble rise speeds of 0 m/s (case 2, Fig. 2); 10^{-7} m/s and 5×10^{-7} m/s. In b, the simulation corresponds to the case a of Fig. 3, with 4 wt% volatiles in both the silicic magma and the basaltic magmas. We now assume a cooling rate of 10^{-7} K/s. Curves are given for bubble rise speeds of 0 m/s (case 2, Fig. 2); 10^{-8} m/s, 3×10^{-8} m/s and 10^{-7} m/s.

ual layer of basalt, and may therefore influence some of the above results relating to bubble separation. We have therefore extended the model to allow for crystal settling, using a second equation of the form of Eq. 10, but now referring to the crystal content of the mixture, following the results of Martin and Nokes [24]. In Fig. 4 we therefore include a second set of curves (solid lines), in which, for illustration, we assume that the crystals settle from the basalt with a settling speed equal to the rise speed of the bubbles. These lines, which may be seen adjacent to the corresponding dashed lines, illustrate that the combined effect of bubble separation and crystal settling from the basalt is to increase the density of the basalt relative to the case in which the bubbles and crystals are assumed to remain in suspension. Although this increase in the density of the basalt is a little smaller than for the case in which crystal settling is ignored (dashed lines), the net effect remains unaltered, the suppression of magma overturn.

4. Analogue laboratory experiments

Our calculations have identified that if the basalt is of sufficiently low viscosity, then bubbles can separate from the melt on a time-scale shorter than the cooling and hence bubble production time. Under such conditions, our model predicts that large-scale overturn may be suppressed. However, for faster cooling rates or bubbles with slower rise speed, large-scale overturn can occur, as originally envisaged by Huppert et al. [2]. In order to test our model, we have conducted a series of analogue laboratory experiments in which small bubbles were produced by electrolysis as an analogue to bubble production by cooling and crystallisation of magma. We used saline solutions mixed with cellulose polymer to create two liquid layers whose viscosity and density could be controlled independently. Dense solutions of relatively low viscosity were introduced into the base of a Plexiglas electrolysis cell, below a layer of less dense but more viscous solution. Small bubbles of diameter 30–50 micron were produced on a sheet of fine nickel gauze cathode at the base of the tank, and these ascended into the lower layer. A series of experiments were conducted using different viscosity and density contrasts over which the initial bubble size remained approximately constant, with the upper layer always more viscous. Our experiments identified that if the lower layer viscosity is smaller than about 1.0 Pa s, then for the given bubble flux the lower layer becomes well-mixed by vigorous bubble convection. Evidence of this mixing included the stirring of a localised streak of dye throughout the lower layer.

For the cases in which the lower layer was mixed vigorously by the bubble convection, we observed a transition in behaviour as the viscosity was reduced. For the higher values of viscosity we observed large-scale overturn and mixing of the two layers of fluid. In contrast, for smaller values of viscosity, there was no large-scale overturn, but bubbles accumulated at the interface to form a foamy layer, which periodically shed plumes of bubbles into the upper layer (cf. [4]; Fig. 3).

We now analyse this transition in mixing behaviour by developing a model of the density evolution of the lower layer of our experimental system, which combines the effects of the bubble production and bubble loss (cf. Section 2). In a series of similar, but simpler experiments, using only one layer of fluid, Cardoso and Woods [23] confirmed that the bubble volume fraction, ϕ say, evolved according to the relation:

$$\frac{d\phi}{dt} = \frac{Q}{hA} - \frac{v\phi}{h} \tag{11}$$

where Q is the volumetric bubble production rate, v is the bubble rise speed, h the depth of the lower layer of liquid and A the area of the tank. Therefore, the lower layer bubble volume fraction, ϕ_l, is expected to evolve according to the relation:

$$\phi_l(t) = \frac{Q}{Av_l}\left(1 - exp\left(-\frac{v_l t}{h_l}\right)\right) \tag{12}$$

If the system evolves to equilibrium, the bubble volume fraction converges to the value $\phi_l(eq) = Q/vA$. This produces a density change in the lower layer $\Delta\rho = \phi_l(eq)\rho_l$, where ρ_l is the liquid density, and where we assume that the bubble density is

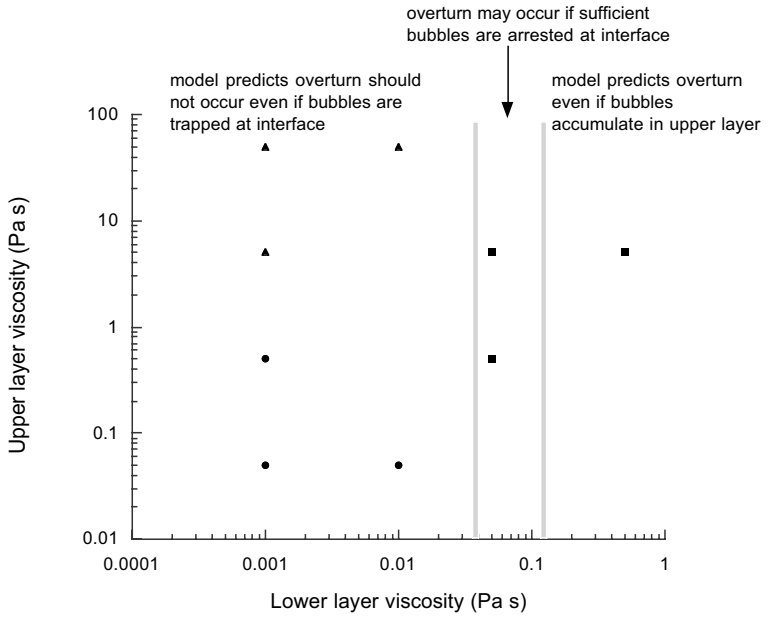

Fig. 5. A summary of the viscosity of the upper and lower layers used in the analogue laboratory experiments. In all experiments, the bubble flux was 67 $mm^3\ s^{-1}$ and the ratio of upper to lower layer density is 1.02. The solid lines correspond to the predictions of Eqs. 13 and 18, which provide bounds on the viscosity of the lower layer for which we anticipate either turnover or stable stratification. The experimental observations are shown with solid markers. Circles and triangles denote experiments in which no overturn occurred, and squares denote experiments in which overturn was observed; these are consistent with the prediction of our model.

negligible compared to the fluid density at laboratory conditions.

To examine the phenomenon of overturn using the present experiments, we need to consider the fate of the bubbles which migrate from the lower layer. In our experiments, the viscosity of the upper layer was much larger than that of the lower layer, and so most bubbles escaping from the lower layer tended to pond at the interface and form a foam. As a result, the density of the upper layer did not evolve significantly (cf. [4]), although plumes of bubble-rich foam did break off and convect into the upper layer. Although the bubble budget in the upper layer is complex, owing to the interaction of the foam and liquid layer, we can compare two end-member models appropriate for the density evolution of the upper layer. First, we assume the density of the upper layer remains unchanged, with all bubbles trapped in the foam layer; second, we assume all bubbles supplied from the lower layer rise into the upper layer and become mixed into that layer.

The first model provides an end-member estimate for determining when overturn cannot occur. Indeed, if:

$$\phi_l(eq) = Q/vA < (\rho_l - \rho_u)/\rho_l \tag{13}$$

where ρ_u is the density of the upper layer of liquid in the experiments, then overturn cannot occur. This condition is shown with a vertical line in the regime diagram of Fig. 5.

The second end-member model provides a bound on conditions under which large-scale overturn is expected to occur. We consider the limit that the upper layer is much more viscous than the lower layer, so that over the time-scale for equilibration of the bubble content of the lower layer, the upper layer essentially retains all bubbles supplied from the lower layer. In this case:

$$\frac{d\phi_u}{dt} = \frac{v_l \phi_l}{h_u} \tag{14}$$

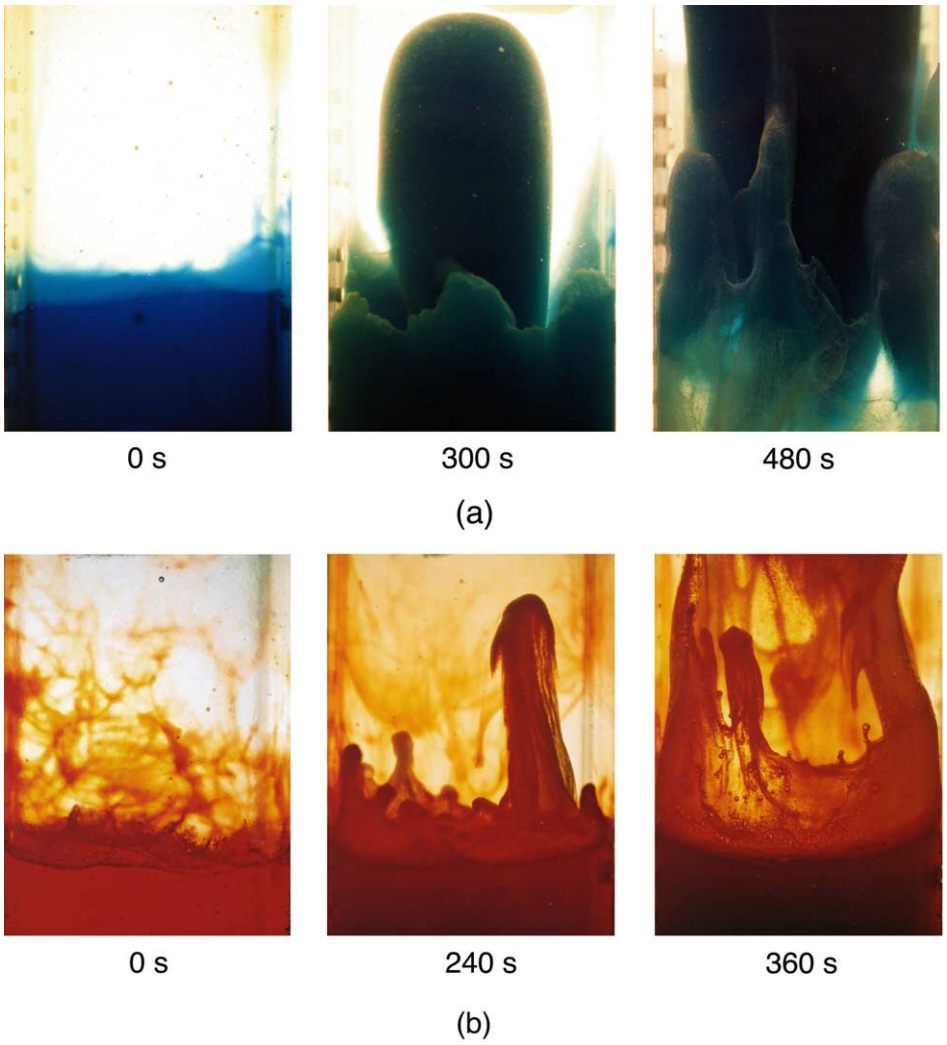

Fig. 6. Observations of the flow regimes identified in laboratory analogue experiments. In each case, the lower layer fluid is dyed, and the tank width is 100 mm. (a) Lower layer viscosity = 0.05 Pa s, upper layer viscosity = 5 Pa s. The density of a convecting lower layer decreases, and its dominant mode of propagation into the upper layer is as a single axisymmetric convecting lobe, which leads to large-scale convective overturn. (b) Lower layer viscosity = 0.05 Pa s, upper layer viscosity = 50 Pa s. Bubbles accumulate at the interface above a convecting lower layer, forming a foam layer, which propagates into the upper layer as discrete bubble plumes.

In the experiments, $h_u \sim h_l$ and so we find that:

$$\phi_u(t) = \frac{Qt}{Ah_l} - \phi_l(t) \tag{15}$$

Therefore, the net change in density between the two layers associated with the bubble transfer between the layers evolves as:

$$\Delta\rho = \rho_l \left(2\phi_l - \frac{Qt}{Ah_l}\right) \tag{16}$$

with a maximum value:

$$\Delta\rho = \frac{Q}{Av_l}(1 - ln2) \tag{17}$$

If the initial density difference between the two layers is smaller than this value:

$$(1-ln2)Q/vA>(\rho_l-\rho_u)/\rho_l \quad (18)$$

then overturn is expected to occur as a result of the bubble generation. This model prediction, as applied to our experiments, is shown as the second vertical line in Fig. 5.

In the intermediate range of initial density differences:

$$\left(\frac{Q}{Av_l}\right)(1-ln2)<(\rho_l-\rho_u)/\rho_l<\left(\frac{Q}{Av_l}\right) \quad (19)$$

the precise mode of mixing is more complex and depends on the foam dynamics (cf. [4]). We have found that in our experiments, the mixing in this intermediate regime tends to fall into the bulk overturn regime. This is consistent with the large viscosity contrast across the two layers which tends to cause formation of a large foam layer at the interface.

For the higher viscosity experiments with lower layer viscosity 0.05 Pa s, we observed large-scale overturn, as would be expected from Eq. 18 for the experimental conditions. Fig. 6a illustrates the nature of the mixing driven by this large-scale overturn. For very low viscosity experiments, 0.001 Pa s, Eq. 13 is satisfied and so we expect that bubble separation will suppress large-scale turnover, again consistent with the observations. Indeed, Fig. 6b illustrates the formation of foam and subsequent mixing of plumes into the upper layer rather than a large-scale overturn event.

5. Discussion

Our work provides a new model with which field observations of magma mixing following intrusion of a dense basic magma into a reservoir charged with more evolved cooler magma may be interpreted. The key principles that we have established through our experimental and theoretical analysis, are:

1. large-scale overturn is likely with high cooling rates and intrusions of relatively viscous juvenile magma into a chamber of volatile saturated silicic magma;
2. if the silicic magma is volatile unsaturated, then the magma is much less compressible and so, prior to any overturn event, the pressurisation associated with the expansion of the basalt might be sufficient to trigger an eruption;
3. magma–volatile separation is likely to be very significant in either a low viscosity lower juvenile layer or with a low cooling rate, and this may suppress large-scale magma overturn. Instead, magma mixing now occurs across the interface, through localised bubble-rich plumes.

These general principles have been established using a simplified model for the evolution of two cooling and crystallising magmas, in which volatiles can exsolve and be resorbed. We have not attempted to simulate specific volcanic eruptions, since for a given eruption there is insufficient data on a number of factors (chamber geometry and size, mode and intensity of convection, magma rheology, compressibility of the host rock, geochemistry of the magmas, etc.). In general, there are a range of magma types which may have a range of different crystallisation sequences with different volatile exsolution laws. We note that it is possible to use more detailed parameterisations of the magma petro-chemistry in this model following the approach of Snyder [15], who used the MELTS algorithm [26] to model the thermal equilibrium of a two-layer magma chamber. A more detailed parameterisation of magma crystallisation and volatile exsolution will not change the broad conclusions of our study and such a level of detail would not be consistent with the other simplifications in building the model. Even with simplified parameterisations, our calculations identify under what general conditions the coupled effects of bubble and crystal production and resorption due to cooling and pressurisation, and bubble and crystal separation by buoyant separation from the melt, will lead to magma mixing and pressurisation.

The impact of bubble separation in suppressing overturn of two viscous liquid layers is shown in

laboratory analogue experiments. We note that while these experiments do not simulate all aspects of the behaviour of magmatic systems and show behaviour more complex than that parameterised in our model, the general principles identified above still hold. For example, in experiments with a very viscous upper layer, a foam can form at the interface between the liquid layers due to bubble separation from the lower layer. In magmatic systems, this foam layer may not form due to viscous coupling between the basaltic and silicic layers or resorption of bubbles at the interface by the silicic magma. However, the purpose of our study is to explore conditions under which overturn may occur, and whether the bubbles form a distinct foam layer, pass into the silicic layer, or are resorbed, the outcome is the same: the lower layer density remains unchanged, and so the bubble separation suppresses overturn. The experiments also show that with more viscous layers channelised flow of bubbles can develop, in contrast to the turbulent suspension that we assume for our model. In viscous crystal-rich magma we expect channelised flow to enhance melt–bubble separation and suppress overturn, compared with the conditions identified in the model.

Although it is difficult to ascertain all the key quantitative parameters for real field examples, there are a number of field observations in which large-scale magma mixing has occurred that are broadly consistent with the principles outlined above. For example, the 1875 eruption of mixed magma from Askja Volcano was preceded by rapid cooling of the basic magma, which had recharged a shallow crustal magma chamber [5]. A high cooling rate was also inferred for the 1991–1995 eruption of mixed magma from Mount Unzen [27]. Hybridisation was also observed in pyroclastic products of the 18.4 ka Cape Riva eruption of Santorini Volcano; here the basic magma was highly crystalline, resulting in a more viscous lower layer and hence a slower bubble rise speed [28].

Similarly, there are observations of cases in which the basalt does not mix fully with the overlying more evolved magma, but volatile gases exsolved from the crystallising basalt separate and rise through the overlying magma. These volatile gases may then be emitted from the volcano during eruption of the evolved overlying magma. For example, mafic inclusions observed in the products of the 1991 eruption of Mount Pinatubo were associated with recharge of a deep magma chamber by a low viscosity basalt, with the eruption preceded by high sulphur gas emissions which originated from the basaltic magma [11]. Similar high sulphur gas emissions have been reported for the 1995–1999 eruption of the Soufriere Hills Volcano, Montserrat [10].

Acknowledgements

We thank R.S.J. Sparks for helpful discussions, and Joan Marti and Don Snyder for constructive reviews. This work was supported by the Leverhulme Foundation, UK and the BP Institute, Cambridge.*[AC]*

Appendix A. Conditions for bubble-driven convection

As the basalt cools and crystallises, it may become volatile saturated, and exsolve volatile bubbles. If the volume concentration of bubbles in the basalt is ϕ, and the temperature anomaly in the magma associated with the cooling and crystallisation is ΔT, then the convective rise speed of a parcel of the bubbly magma scales as:

$$u \sim \frac{(\phi \Delta \rho - \alpha \Delta T) g h^2}{\mu} \tag{A1}$$

where $\Delta\rho$ is the density contrast between the bubbles and magma, μ is the magma viscosity (cf. [8]), and α is the thermal expansion coefficient, including the effects of liquid–solid phase change. With typical magma compositions it has been shown that $\phi\Delta\rho \gg \alpha\Delta T$ [2] and hence the density change associated with the bubbles dominates the effects of cooling and crystallisation of the magma [8]. In order to estimate the bubble volume fraction ϕ in Eq. A1, we note that if Q is the bubble production rate per unit area, then, in the absence of

convection:

$$\phi \sim Q/v_s \tag{A2}$$

Vigorous bubble-driven convection will develop in the magma [8] if the rise speed of bubbles is much smaller than the convective velocity of a parcel of buoyant magma:

$$v_s \ll u \tag{A3}$$

Combining Eq. A1–A3 we deduce that the basalt will convect vigorously if the bubble production rate per unit area satisfies:

$$Q \gg Q_c = \frac{\mu v_s^2}{\Delta \rho g h^2} \tag{A4}$$

The bubble production rate depends on the rate of cooling and crystallisation of the basalt and the solubility of volatiles in the melt. The mass of dissolved gas in the magma may be written (Eq. 1) $n_i = sP^{1/2}(1-x_i)$, and so the rate of bubble production per unit area has the form:

$$h_i dn_i/dt = h_i sP^{1/2}(dx_i/dT)(dT/dt) \tag{A5}$$

where h_i is the layer depth. This has value: $h_i\ dn_i/dt \sim 10^{-4}\ dT/dt$.

For cooling rates of order 10^{-6}–10^{-8} K/s we expect a bubble flux of order 10^{-8}–10^{-10} in a 100-m-deep layer. In contrast, for a magma of viscosity 10 Pa s and bubble rise speed of 50 μm/s, Eq. A4 suggests that Q_c has the value of order 10^{-16}. We deduce that $Q_c \ll h_i dn_i/dt$ and so we expect vigorous bubble convection in the basaltic layer.

References

[1] J.C. Eichelberger, D.G. Chertkoff, S.T. Dreher, C.J. Nye, Magmas in collision: rethinking chemical zonation in silicic magmas, Geology 28 (2000) 603–606.

[2] H.E. Huppert, R.S.J. Sparks, J.S. Turner, Effects of volatiles on mixing in calc-alkaline magma systems, Nature 297 (1982) 554–560.

[3] D. Snyder, S.R. Tait, Replenishment of magma chambers: comparison of fluid-mechanic experiments with field relations, Contrib. Mineral. Petrol. 122 (1995) 230–240.

[4] N. Thomas, S. Tait, T. Koyaguchi, Mixing of stratified liquids by the motion of gas bubbles: application to magma mixing, Earth Planet. Sci. Lett. 115 (1993) 161–175.

[5] H. Sigurdsson, R.S.J. Sparks, Petrology of rhyolitic and mixed ejecta from the 1875 eruption of Askja, Iceland, J. Petrol. 22 (1981) 41–84.

[6] A.T. Anderson, Magma mixing: petrological process and volcanological tool, J. Volcan. Geotherm. Res. 1 (1976) 1–33.

[7] A. Bond, R.S.J. Sparks, The Minoan eruption of Santorini, Greece, J. Geol. Soc. London 132 (1976) 1–16.

[8] S.S.S. Cardoso, A.W. Woods, On convection in a volatile-saturated magma, Earth Planet. Sci. Lett. 168 (1999) 301–310.

[9] J.C. Eichelberger, Vesiculation of mafic magma during replenishment of silicic magma reservoirs, Nature 288 (1980) 446–450.

[10] M.D. Murphy, R.S.J. Sparks, J. Barclay, M.R. Carroll, T.S. Brewer, Remobilization of andesite magma by intrusion of mafic magma at the Soufriere Hills, Montserrat, West Indies, J. Petrol. 41 (2000) 21–42.

[11] J.S. Pallister, R.P. Hoblitt, A.G. Reyes, A basalt trigger for the 1991 eruptions of Pinatubo volcano?, Nature 356 (1992) 426–428.

[12] A. Folch, J. Marti, The generation of overpressure in felsic magma chambers by replenishment, Earth Planet. Sci. Lett. 163 (1998) 301–314.

[13] S.R. Tait, C. Jaupart, S. Vergniolle, Pressure, gas content and eruption periodicity of a shallow crystallizing magma chamber, Earth Planet. Sci. Lett. 92 (1989) 107–123.

[14] H.E. Huppert, R.S.J. Sparks, J.S. Turner, Replenished magma chambers: effects of compositional zonation and input rates, Earth Planet. Sci. Lett. 57 (1982) 345–357.

[15] D. Snyder, Thermal effects of the intrusion of basaltic magma into a more silicic magma and implications for eruption triggering, Earth Planet. Sci. Lett. 175 (2000) 257–273.

[16] Y.S. Touloukian, W.R. Judd, R.F. Roy, Physical Properties of Rocks and Minerals, Vol. 1, Hemisphere, New York, 1981, 548 pp.

[17] J.R. Holloway, J.G. Blank, Application of experimental results to C-O-H species in natural melts, Rev. Mineral. 30 (1994) 187–230.

[18] H.E. Huppert, R.S.J. Sparks, The generation of granitic magmas by the intrusion of basalt into continental crust, J. Petrol. 29 (1988) 599–624.

[19] S. Blake, Volatile saturation during the evolution of silicic magma chambers as an eruption trigger, J. Geophys. Res. 89 (1984) 8237–8244.

[20] S.M. Bower, A.W. Woods, On the influence of magma chambers in controlling the evolution of explosive volcanic eruptions, J. Volcan. Geotherm. Res. 86 (1998) 67–78.

[21] T.W. Sisson, T.L. Grove, Temperatures and H_2O con-

tents of low-MgO high-alumina basalts, Contrib. Mineral. Petrol. 113 (1993) 168–184.
[22] T.W. Sisson, G.D. Layne, H_2O in basalt and basaltic andesite glass inclusions from four subduction-related volcanoes, Earth Planet. Sci. Letts. 117 (1993) 619–635.
[23] S.S.S. Cardoso, A.W. Woods, Interfacial turbulent mixing in stratified magma reservoirs, J. Volcanol. Geotherm. Res. 73 (1996) 157–175.
[24] D. Martin, R. Nokes, Crystal settling in a vigorously convecting magma chamber, Nature 332 (1988) 534–536.
[25] R. Jarvis, A.W. Woods, The nucleation, growth and settling from a turbulently convecting fluid, J. Fluid Mech. 273 (1994) 83–107.
[26] M.S. Ghiorso, Algorithms for the estimation of phase stability in heterogeneous thermodynamic systems, Geochim. Cosmochim. Acta 58 (1994) 5489–5501.
[27] D. Venesky, M.J. Rutherford, Petrology and Fe-Ti oxide reequilibration of the 1991 Mount Unzen mixed magma, J. Volcanol. Geotherm. Res. 89 (1999) 213–230.
[28] T.H. Druitt, L. Edwards, R.M. Mellors, D.M. Pyle, R.S.J. Sparks, M, Lanphere, M. Davies, B. Barriero, Santorini Volcano. Geol. Soc. London Memoir 19, 1999, 162 pp.